Economic and simple system to combine single-spot photolysis and whole-field fluorescence imaging

Nadia Jaafari [1 2], Mark Henson [3], Jeremy Graham [3], Marco Canepari [1 2 *]

[1] *GIN, Grenoble Institut des Neurosciences INSERM : U836 , Université Joseph Fourier - Grenoble I , CHU Grenoble , CEA : DSV/IRTSV , UJF - Site Santé La Tronche BP 170 38042 Grenoble Cedex 9, FR*

[2] *LIPhy, Laboratoire Interdisciplinaire de Physique CNRS : UMR5588 , Université Joseph Fourier - Grenoble I , 621 Avenue Centrale, 38041 Saint-Martin-d'Hères Grenoble, FR*

[3] *Fluorescence Imaging, Electrophysiology and Microscopy Cairn Research Limited , Graveney Road, Faversham Kent, ME13 8UP, GB*

* Correspondence should be addressed to: Marco Canepari <marco.canepari@ujf-grenoble.fr >

Abstract

In the recent years, the use of light emitting diodes (LEDs) has become commonplace in fluorescence microscopy. LEDs are economical, easy to couple to commercial microscopes and provide powerful and stable light that can be triggered by TTL pulses in the range of tens of microseconds or shorter. LEDs are usually installed on the epifluorescence port of the microscope to obtain whole field illumination which is ideal for fluorescence imaging. In contrast, photolysis or channelrhodopsin stimulation often requires localised illumination, typically achieved using lasers. Here we show that insertion of a long-pass (>411 nm) filter with appropriately sized pinhole in the epifluorescence pathway, combined with dual UV/visible illumination, can produce efficient whole field visible illumination and spot UV illumination of 15–20 μm. We tested our system by performing calcium imaging experiments combined with L-glutamate or NMDA photo-release in hippocampal neurons from brain slices or dissociated cultures, demonstrating the ability to obtain local activation of NMDA receptors exclusively in the illuminated spot. The very inexpensive and simple system that we report here will allow many laboratories with limited budget to run similar experiments in a variety of physiological applications.

Author Keywords Photolysis ; Calcium imaging ; LED illumination ; Epifluorescence microscope

Introduction

For functional imaging applications, solid state lasers and light emitting diodes (LEDs) are progressively replacing the arc lamps or lamp-based illumination systems that were routinely used for more than three decades.[1] Modern solid state lasers provide high power, stable and monochromatic illumination, but despite typically delivering fewer photons to the sample, several advantages make LEDs preferable in many situations. First, LEDs are cheaper, more compact and easier to control; they can be powered by a constant current source and triggered by TTL pulses with microsecond precision. Second, LEDs produce incoherent light over a wide range of angles which can be easily collimated and mounted onto the standard epifluorescence port of commercial microscopes to obtain nearly uniform illumination of the whole visual field, which is ideal for fluorescence imaging using a camera. Third, LEDs are safer and do not produce the laser speckle associated with coherent light sources, while they can still be mounted in cascade to obtain multi-colour illumination. The light of LEDs, although less powerful than that of lasers, is bright enough not only for fluorescence excitation but also for photo-stimulation, for instance for activation of Channelrhodopsin (ChR)[2] or for molecular photo-release from caged compounds.[3] However, some applications require local photo-stimulation and therefore illumination from relatively small spots. Diffraction limited spots of <1 μm can only be generated using a laser.[4] Nevertheless, lasers are more difficult to work with and, because they produce a tight collimated beam, they require more stringent safety procedures, which are not always convenient when working with physiological preparations. Thus, it is extremely useful to explore to what extent local photo-stimulation can be achieved, in a simpler and cheaper way, using LED illumination. To investigate this possibility, we used the flexibility of the Olympus BX microscope, which has an adjustable field stop designed to reduce the field of fluorescence illumination. We replaced this field stop with a device where we alternatively mounted pinholes of different sizes, drilled through 411 nm long pass filters. In this way, we could combine local UV illumination and whole-field visible illumination. As the light intensity decreased with the diameter of the UV spot, we found that the intensity is still >10% for a spot of 15–20 μm and sufficient to obtain significant photolysis using short pulses from commonly used 4-Methoxy-7-nitroindolinyl (MNI) caged compounds.

Materials and Methods

Experiments were performed using an Olympus BX51 microscope equipped with a 60X/1.0 NA Nikon objective. A dual-port coupler for LEDs, equipped with a 409nm dichroic mirror (FF409, Semrock, Rochester, New York) was mounted on the epifluorescence port the microscope. A 365 nm LED controlled by an OptoFlash (CAIRN Research Ltd., Faversham, UK) and 470 nm LED controlled by an OptoLED (also from Cairn) were mounted on the two ports of the coupler and used for uncaging and fluorescence excitation respectively. A silica condenser lens was used with the ultraviolet LED which allowed full-field illumination if required. Alternative optics to

concentrate light over a smaller area may allow throughput improvements in future, but the purpose of this paper was to investigate the diffractive losses associated with masking a full-field beam. To manufacture “long-pass” (LP) pinholes, holes of 100 μm, 150 μm, 200 μm and 300 μm were drilled by Small Hole Drilling s.r.o. (Nám nad Oslavou, Czech Republic) on 411 nm LP Wratten gelatin filters (411 WY 75, Comar, Cambridge, UK) and mounted on a black plastic ring. The ring, shown in the bottom picture of Fig. 1(a) on the right, was inserted in a custom-made slider (bottom picture of Fig. 1(a) left) to replace the field-stop of the Olympus BX51 microscope as illustrated in the top picture of Fig. 1(a). The position of the pinhole, relative to the specimen, could be adjusted with two screws, in our case in the middle of the field of view of the CCD camera used for imaging. This device is now commercially available from Cairn. The LED light downstream of the LP pinhole was directed to the objective [Fig. 2(b)] using a 506 nm dichroic mirror (FF506, Semrock) and fluorescence emission was filtered at 510 ± 42 nm, demagnified by 0.5X and acquired using a NeuroCCD-SM camera (RedShirtImaging LLC, Decatur, GA) at 1000 frames/s. Calcium fluorescence signals were expressed as fractional changes of fluorescence ($\Delta F/F$). Hippocampal slices (250 μm thick) were prepared from a 32 postnatal days old C57Bl6 mouse using a VF-200 compresstome (Precisionary Instruments, Greenville, NC). Experiments were approved by the Isere prefecture (Authorisation n. 38 12 01) and the specific protocol (n. 197) by the ethics committee of the Grenoble Institute of Neuroscience. Hippocampal cell cultures were prepared from embryonic day 18 (E18) rat embryos by the laboratory of Yves Goldberg as described in Belly et al.[5] and used after two weeks. The extracellular solution used in our recordings contained (mM): 125 NaCl, 26 $NaHCO_3$, 20 glucose, 3 KCl, 1 NaH_2PO_4, 2 $CaCl_2$ and 0.001 tetrodotoxin bubbled with 95% O_2 and 5% CO_2. The intracellullar solution contained (mM): 125 $KMeSO_4$, 5 KCl, 8 $MgSO_4$, 5 Na_2-ATP, 0.3 Tris-GTP, 12 Tris-Phosphocreatine, 20 HEPES, adjusted to pH 7.35 with KOH. Calcium indicators, either Oregon Green 5N (OG5N) or Oregon Green BAPTA-1 (OGB1) were purchased from Invitrogen (Carlsbad, CA) and added at a concentration of 500μM to the internal solution. Patch-clamp recordings were made using a Multiclamp amplifier 700A (Molecular Devices, Sunnyvale, CA). Photo-release of L-glutamate or *N*-Methyl-D-aspartic acid (NMDA) was produced from the caged compounds MNI-glutamate [6] and MNI-NMDA [7], purchased from Tocris (Bristol, UK). Caged compounds were dissolved at 1 mM concentration in extracellular solution and applied locally near the cell with a large pipette to obtain a uniform concentration in the area of photolysis while avoiding light absorption in the pathway from the objective to the cell.

Results

The goals of this work were: 1. to quantify the intensity and spatial distribution of UV light through LP pinholes; 2. to test whether UV light through LP pinholes could produce efficient and localised photolysis from commercial caged compounds in simple proof-of-principle uncaging/Ca^{2+} experiments in cellular preparations. Fig. 1(c) shows images from a fluorescent slide, illuminated either at 470 nm or at 365 nm, without any pinhole or with the 100 μm, 150 μm, 200 μm and 300 μm diameters pinholes. These images illustrate that the UV illumination is concentrated in spots of ~10 μm, 15 μm, 20 μm and 30 μm respectively. To quantify the spatial profile of the UV illumination with the pinholes, we plotted the light intensity in the central row, normalised to the maximal intensity without the pinhole [Fig. 1(d) left] and to the maximal intensity with the pinholes [Fig. 1(d) right]. The first plot shows that the light intensity with the pinholes, reduced by diffraction, is respectively 5%, 10%, 15% and 21% of the maximal intensity without the pinhole, including a background of 3% of bleedthrough passing through the gelatin filter. The second plot shows that for the four pinholes, the diameter within which the light intensity is >50 % of its maximum is 6 μm, 11.5 μm, 14.5 μm and 20.5 μm respectively. The power of our 365 nm LED at the back-aperture of the objective is >50 mW. This power produces very efficient photolysis from MNI-caged compounds with light exposures >100 μs. Thus, we expected to obtain efficient photolysis with light pulses >1-ms through the 150–200 μm pinholes. To test this hypothesis in a biological application, we filled a CA1 hippocampal pyramidal neuron from a brain slice with the low affinity indicator OG5N (K_d = 35 μM [8]) and we measured the $\Delta F/F$ Ca^{2+} signal via NMDA receptors (NMDARs) generated by L-glutamate uncaging with pulses of 1–4 ms using the 150 μm LP pinhole [Fig. 2(a)]. To mimic a physiological scenario, we uncaged L-glutamate onto a spot in the main apical dendrite located ~100 μm from the soma where Shaffer collateral synapses are expected to form. We then compared the spatial distribution of the $\Delta F/F$ signal generated by a 3 ms UV pulse through the 150 μm LP pinhole with that generated by a 200 μs UV pulse without pinhole [Fig. 2(b) and SupplementaryMovie1]. As shown in Fig. 2(c), the amplitude of the $\Delta F/F$ signal in the two cases is similar in the photolysis spot (dotted circle) but Ca^{2+} elevation outside the spot is observed only without the LP pinhole, in agreement with the larger somatic current recorded with the patch clamp electrode [Fig. (2c) bottom-left]. A Ca^{2+} elevation outside the spot was however still observed with the LP pinhole for pulses >5 ms (data not shown). This phenomenon could be due to the leak of UV light through the gelatin filter and to the L-glutamate diffusion after photo-release. Thus, to quantitatively test photolysis localisation with short pulses, we performed experiments of NMDA photo-release in dissociated cultures. For our purpose, experiments in cultures have two advantages. First, the caged compound applied extracellularly equilibrates by diffusing in free space and it is uniform over the area of UV illumination. Second, also the released NMDA equilibrates by diffusion in the free space-interacting exclusively with NMDARs and not to other receptors or to glutamate transporters. The hippocampal cell in Fig. 2(d) was filled with 500 μM of OG5N. In the image of the recording position on the left, we added a dark shadow to indicate the region of the UV spot and selected three regions of interest (A, B and C) in the middle, in the periphery and outside the spot. Fig. 2(e) shows the NMDA current and the associated $\Delta F/F$ signals in regions A-C following a 2 ms UV pulse through the 200 μm. The spatial profiles of $\Delta F/F$, averaged over two time windows (11–18 ms and 59–88 ms) are illustrated in Fig. 2(f) using a colour scale. The spatial profile of activated NMDARs does not necessarily coincide with that of photolysis

because NMDARs can be also activated by lateral diffusion of NMDA from the uncaging site. In addition, the spatial profile of Ca^{2+} fluorescence evolves following diffusion of the indicator bound to Ca^{2+} . This component, however, depends on the affinity of the indicator since Ca^{2+} unbinding from high affinity indicators is slower.[8] Thus, to appreciate this effect, we repeated the same experiment in another cell [Fig. 2(g)] filled with 500 μM of the high affinity indicator OGB1 (Kd = 200 nM [9]). As shown in the traces of Fig. 2(h) and from the averaged Δ*F/F* profiles in Fig. 3(i), the Ca^{2+} bound to OGB1 is initially observed exclusively in the spot and it later diffuses outside the spot, an effect less evident with OG5N. We further analyse the UV illumination profile and Ca^{2+} fluorescence averaged over the two time windows of Fig. 2(f) and Fig. 2(i) in the rectangular region depicted in Fig. 2(j) [left]. In particular, we averaged light intensities over the *y* axis and plotted the results over the *x* axis as a function of the distance from the point of maximal UV illumination. This analysis allows a comparison of distributions of UV light intensity and of Δ*F/F* signals in the two time windows. The *x*-profiles of Δ*F/F* signals at 11–18 ms after UV exposure remarkably match the profile of UV illumination. In contrast, Δ*F/F* signals are clearly present outside the UV spot at 59–88 ms after UV exposure. Because the non-co-localised signal is much larger with OGB1, we conclude that this effect is due to the diffusion of the bound indicator and not to the photo-released NMDA. The same analysis also indicates that the contribution of NMDA photo-release by the UV leak through the gelatin filter is negligible. We can therefore conclude that the profile of NMDARs activation matches that of the UV spot that we created with the pinhole. The time-course of the Δ*F/F* signal in these two cells is illustrated in the Supplementary Movie2.

Discussion

Combining photo-stimulation with Ca^{2+} imaging [8] or voltage imaging [10] is important to address a variety of physiological questions. Some experiments can be performed by illumination of the whole field of view using either a flash-lamp [11] or an LED. In contrast, local photo-stimulation is typically achieved using lasers. Thus, one-photon [4] or two-photon [12] laser photo-stimulation permits illumination of spots <1 μm, i.e. an area close to that of a dendritic spine. The implementation of laser photo-stimulation, however, can be expensive and difficult to combine with other illumination systems used for fluorescence excitation. For this reason we explored to what extent usefully local photo-stimulation could be achieved using a simple and economic multicolour LED system that is simultaneously used for fluorescence excitation. We implemented this solution by inserting a LP filter with a pinhole in the illumination pathway. The localisation of small spots is less precise than would be predicted by the magnification of the objective lens and epi-condenser optics and is instead limited by diffraction which also reduced the light intensity in the illuminated area. The practical question we addressed was therefore to find out the smallest spot size that could allow efficient and local photolysis. We have shown here that this could be achieved with MNI-caged compounds in spots of 15–20 μm using illumination pulses of 1–4 ms. The size of this spot is sufficiently small for many photolysis applications, including extra-synaptic activation of receptors or local activation of intracellular pathways. The principle of drilling a pinhole in a LP filter can be extended to longer wavelengths permitting local ChR stimulation and imaging with a combination of blue and green or red light illumination. In conclusion, this solution is now commercially available and we foresee that it will be adopted by several laboratories.

Acknowledgements:

We thank Dr. Yves Goldberg and Dr. José Martínez Hernández for providing the hippocampal cultured used in our experiments, Philippe Moreau for technical help and Jean-Claude Vial for useful discussions. All experiments were performed at the “Laboratoire Interdisciplinaire de Physique” of the Joseph Fourier University. This work was supported by the *Agence Nationale de la Recherche* (Grant *Voltimagmicro*, program *Emergence-10* and Labex *Ion Channels Science and Therapeutics*).

References:

- 1 . Thomson LA , Hageage GL . Evaluation of excitation light sources for incident immunofluorescence microscopy . Appl Microbiol . 30 : (4) 616 - 624 1975 ;
- 2 . Zhang F . Channelrhodopsin-2 and optical control of excitable cells . Nat Methods . 3 : (10) 785 - 792 2006 ;
- 3 . McCray JA , Trentham DR . Properties and uses of photoreactive caged compounds . Annu Rev Biophys Biophys Chem . 18 : 239 - 270 1989 ;
- 4 . Trigo FF , Corrie JE , Ogden D . Laser photolysis of caged compounds at 405 nm: photochemical advantages, localisation, phototoxicity and methods for calibration . J Neurosci Methods . 180 : (1) 9 - 21 2009 ;
- 5 . Belly A . CHMP2B mutants linked to frontotemporal dementia impair maturation of dendritic spines . J Cell Sci . 123 : (17) 2943 - 2954 2010 ;
- 6 . Canepari M . Photochemical and pharmacological evaluation of 7-nitroindolinyl-and 4-methoxy-7-nitroindolinyl-amino acids as novel, fast caged neurotransmitters . J Neurosci Methods . 112 : (1) 29 - 42 2001 ;
- 7 . Palma-Cerda F . New caged neurotransmitter analogs selective for glutamate receptor subtypes based on methoxynitroindoline and nitrophenylethoxycarbonyl caging groups . Neuropharmacology . 63 : (4) 624 - 634 2012 ;
- 8 . Canepari M , Odgen D . Kinetic, pharmacological and activity-dependent separation of two Ca^{2+} signalling pathways mediated by type 1 metabotropic glutamate receptors in rat Purkinje neurons . J Physiol . 573 : (1) 65 - 82 2006 ;
- 9 . Maravall M . Estimating intracellular calcium concentrations and buffering without wavelength ratioing . Biophys J . 78 : (5) 2655 - 2667 (200)
- 10 . Vogt KE . Combining membrane potential imaging with L-glutamate or GABA photorelease . PLoS One . 6 : (10) e24911 - 2012 ;
- 11 . Rapp G . Flash lamp-based irradiation of caged compounds . Methods Enzymol . 291 : 202 - 222 1998 ;
- 12 . Pettit DL . Chemical two-photon uncaging: a novel approach to mapping glutamate receptors . Neuron . 19 : (3) 465 - 471 1997 ;
- 13 . Canepari M , Mammano F . Imaging neuronal calcium fluorescence at high spatio-temporal resolution . J Neurosci Methods . 87 : (1) 1 - 11 1999 ;

Figure 1

LED illumination with LP pinholes. (a) Picture of a device designed for Olympus BX microscopes to insert and position LP pinholes in the epifluorescence pathway (left); gelatin filters where the pinholes were drilled glued on plastic rings and placed in the device (right). (b) Scheme of the 365/470 nm illumination; LP pinholes produce whole field visible illumination and spot UV illumination. (c) Illumination patterns at 470 nm and 365 nm with a 60X objective (top); patterns correspond to illumination without pinholes and with 100 μm, 150 μm, 200 μm and 300 μm pinholes; scale bar 20 μm. (d) Illumination profiles of a pixel line in the middle row of the image; left: profiles normalised to image without pinhole; right: profiles normalised to their maxima; spot diameters with more than 50% of the light intensity (double arrows) were 6 μm, 11.5 μm, 14.5 μm and 20.5 μm.

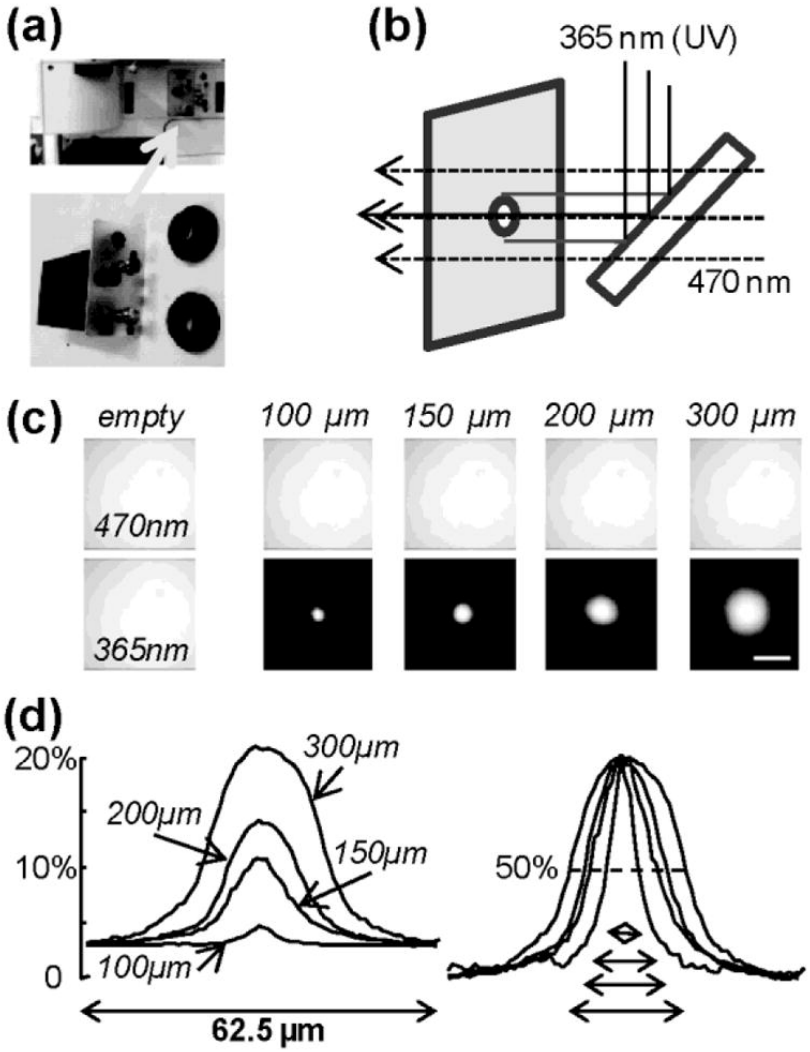

Figure 2

Simultaneous photolysis and Ca^{2+} imaging. (a) Reconstruction of a hippocampal neuron filled with 500 μM OG5N; in the recording position image below the UV spot (150 μm pinhole) represented by a dotted circle; red and black traces are respectively the Δ*F/F* Ca^{2+} signals in the red square and the somatic currents associated with UV flashes of 1, 2, 3 and 4 ms uncaging glutamate. (b) Spatial distributions of Δ*F/F* superimposed to the image represented in a colour scale during the period of 150–200 ms after a 3 ms pinhole UV flash (left) and after a 0.2 ms whole field UV flash (right). (c) Δ*F/F* signals after the pinhole UV flash (red traces) and after the whole field UV flash (green traces) in the three regions A–C indicated on the left image; correspondent somatic currents indicated below. (d) Reconstruction of a cultured hippocampal neuron filled with 500 μM OG5N; in the recording position image on the right the position of the UV spot (200 μm pinhole) is represented by a gray shadow; the coloured frames indicate three regions of interest (A, B and C) in the middle of the spot, in the periphery and outside the spot. (e) Δ*F/F* associated with a UV flash (occurring at t=0) uncaging NMDA from the regions A–C in d; somatic recording of the NMDA current below (black trace); duration of UV flash 2 ms. (f) Spatial distribution of Δ*F/F* superimposed to the image represented in a colour scale during the periods of 11–18 ms and 59–88 ms after the UV flash (t=0). (g–i) Same as A–C in another cultured hippocampal neuron filled with OGB1. (j) Another picture of the 200 μm pinhole with a rectangle of 40 X 16 pixels (*x* X *y* axes); the dotted line represents the profile of UV light intensity averaged over the 16 pixels on *y* axis as a function of the distance of the pinhole centre; below, superimposed to the UV light intensity profile, the profiles of normalized Δ*F/F* during the periods of 11–18 ms and 59–88 ms after the UV flash (t=0) as a function of the distance of the pinhole centre.